EurJOC
European Journal of Organic Chemistry

A Journal of ChemPubSoc Europe

Accepted Article

Title: 3,7-bis(N-methyl-N-phenylamino)phenothiazinium salt: improving synthesis and understanding aggregation behavior in solution

Authors: Martina Tiravia, Federica Sabuzi, Martina Cirulli, Silvia Pezzola, Graziano Di Carmine, Daniel Oscar Cicero, Barbara Floris, Valeria Conte, and Pierluca Galloni

To be cited as: *Eur. J. Org. Chem.* 10.1002/ejoc.201900504

Link to VoR: http://dx.doi.org/10.1002/ejoc.201900504

Supported by
ACES Asian Chemical Editorial Society

WILEY-VCH

WILEY-VCH

FULL PAPER

3,7-bis(*N*-methyl-*N*-phenylamino)phenothiazinium salt: improving synthesis and understanding aggregation behavior in solution

Martina Tiravia,[a]† Federica Sabuzi,[a]† Martina Cirulli,[a,b] Silvia Pezzola,[c] Graziano Di Carmine,[d] Daniel Oscar Cicero,[a] Barbara Floris,[a] Valeria Conte[a] and Pierluca Galloni*[a]

to the memory of Prof. Cinzia Chiappe, great friend and chemist

Abstract: In this paper the optimization of the synthesis of 3,7-bis(*N*-methyl-*N*-phenylamino)phenothiazinium chloride with a detailed analysis of reaction parameters, *i.e.* solvent, temperature, amount of amine, as well as addition of a non-nucleophilic base, is presented. Spectroscopic, electrochemical and computational data show that the presence of the two phenyl rings, directly bound on the PTZ^+ core, inhibits the aggregation ability of the salt at concentrations up to 10^{-3} M. Furthermore, the introduction of an aromatic group in phenothiazinium-based molecules appears strategic to introduce other useful functionalities, thus opening new opportunities in the drug design/discovery research field.

Introduction

3,7-Dimethylaminophenothiazinium chloride, commonly known as Methylene Blue (**MB**), is an outstanding compound because of its plentiful potential applications, low toxicity and favorable electrochemical proprieties. However, although **MB** may be applied in several fields, which ranges from green energy [1-3] (*i.e.* solar panels) to pharmaceutical [4-19] (*i.e.* anti-septic and photo-therapy drugs), its usage is still limited because of the tricky synthetic and purification procedures needed as well as the spontaneous and disadvantageous aggregation in solution. Nowadays, the synthesis requires five steps (Scheme 1), where the most critical ones are the intermediate deprotonation (Scheme 1, step 5) and the product purification, which is laborious and cannot be standardized.

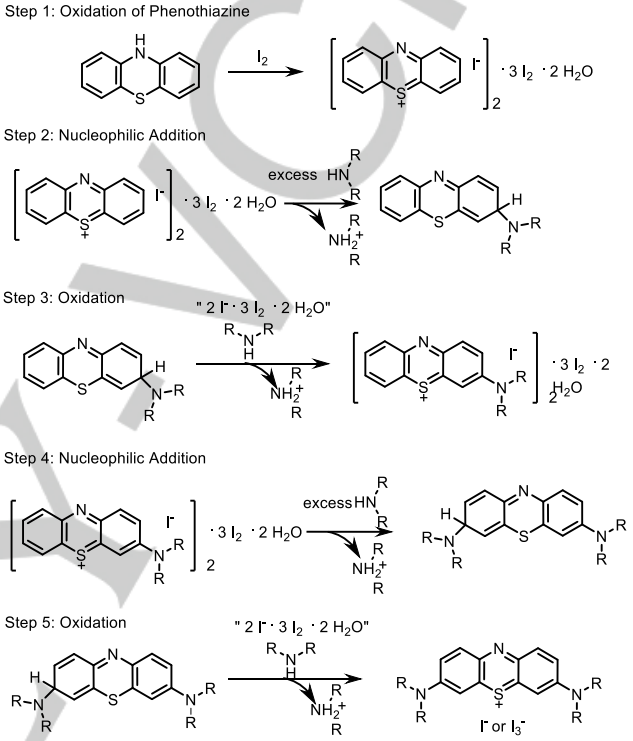

Scheme 1. Structure of 3,7- bis(*N*-methyl-*N*-phenylamino)phenothiazinium iodide.

Moreover, aggregates formation hinders application in DSSCs because it causes acceleration of charge-recombination process, lowering the overall efficiency of the cell [20] and a similar effect can be observed in the photodynamic therapy, where aggregation reduces the singlet oxygen quantum yield.[21]

Despite the most studied phenomenon is the **MB** dimerization, other aggregation forms are possible, such as n-aggregation[22] and anion-cation separation.[23]

To deeply investigate how π-π interactions may be prevented, in this work we propose a detailed computational and experimental analysis of a PTZ^+ derivative, *i.e.* 3,7-bis(*N*-methyl-*N*-phenylamino)phenothiazinium salt (**1**) (Scheme 2). In particular, the presence of phenyl-groups might display a large number of advantages, such as the superior steric hindrance to disfavor aggregation, the possibility to tune the electrochemical and photo-physical properties as well as to introduce new substituents on the ring easily.

The study takes into account the effects of solvent polarity, pH and ionic-strength on the aggregation of both, **MB** and **1**.

[a] Dr. M, Tiravia, Dr. F, Sabuzi, Prof. D. O, Cicero, Prof. B, Floris, Prof. V, Conte and Prof. P, Galloni
Department of Chemical Sciences and Technologies
University of Rome Tor Vergata
Via della Ricerca Scientifica snc, 00133 Rome, Italy
E-mail: galloni@scienze.uniroma2.it
http://stc.uniroma2.it/professori-associati/?cn-entry-slug=pierluca-galloni
[b] Dr. M, Cirulli
School of Biological and Chemical Sciences
Queen Mary University of London
Mile End Road, London E1 4NS, United Kingdom
[c] Dr. S, Pezzola
BT-InnoVaChem srl
Via della Ricerca Scientifica snc, 00133 Rome, Italy
[d] Dr. G, Di Carmine
Department of Chemical and Pharmaceutical Sciences
University of Ferrara
Via L. Borsari 4, 44121 Ferrara, Italy
† These authors contributed equally.
Supporting information for this article is given via a link at the end of the document.

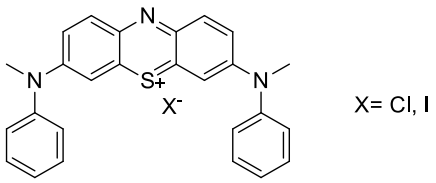

Scheme 2. Structure of 3,7-bis(*N*-methyl-*N*-phenylamino)phenothiazinium salt (**1**).

Furthermore, linking our experience in synthesis optimization[24-31] together with a broad investigation of literature data, we have also optimized a one-pot reaction, aimed to overcome the aforementioned synthetic troubles, thus improving the application of this class of compounds as dyes in the solar cells field, in the photodynamic therapy, likewise to study their interactions with DNA and proteins.[32]

Results and Discussion

DFT Calculation

In order to understand if steric hinderance in positions 3 and 7 of the phenothiazine core could have a key role in preventing aggregation, DFT calculations of dimeric forms of **MB** and **1** have been performed, using WB97XD functional and 6-31G+(d,p) basis set.[33] As a matter of fact, results indicated that the π-stacked dimer of **MB** (Figure 1) converged to a minimum of energy, whereas the dimeric form of **1** did not. Moreover, DFT analysis using the B3LYP/6-31G+(d,p) has pointed out that several conformations of **1** are possible: phenyl rings can be accommodated perpendicularly to the polycyclic ring (Figure 2, conformer *A*), in equatorial-like conformation (Figure 2, conformer *C*) or one perpendicular and the other in the equatorial-like conformation with respect to the PTZ^+ core (Figure 2, conformer *B*). DFT calculations showed that the energetic gap in the *vacuum* among the three conformers is negligible (~0.2 kcal/mol), thus suggesting an equilibrium. However, the activation energies for rotational transitions ($\Delta E^{\neq}_{A\text{-}B}$ and $\Delta E^{\neq}_{B\text{-}C}$) in the *vacuum* resulted too high for the interconversion (Table 1).

To evaluate how the solvent could affect the conformers stability and the transition states energy, the same calculations has been performed introducing an infinite *continuum* dielectric around the cavities containing the molecules (Table 2). In particular, calculations were performed in two conventional solvents, such as chloroform and water.

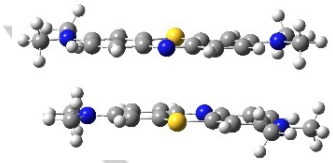

Figure 1. Geometry optimization of **MB** (left) dimers in the *vacuum*, using WB97XD functional.

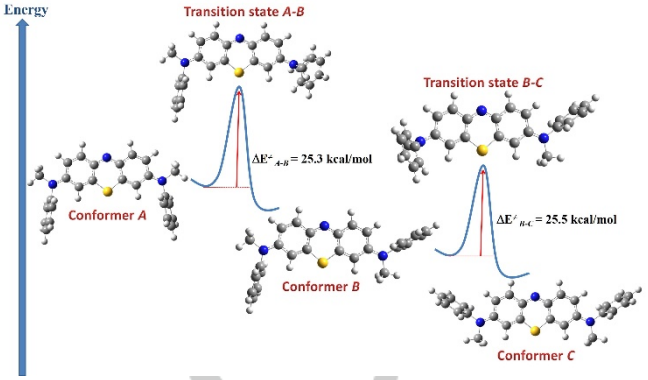

Figure 2. Energy diagram of the conformers and the rotational transition states for **1** in the *vacuum*.

The energetic gap between conformers *A* and *B* ($\Delta E_{A\text{-}B}$) seems not to be affected by solvent, while conformer *C* showed higher stability with respect to *B*, both in chloroform ($\Delta E_{B\text{-}C}$ ($CHCl_3$) = 3.8 kcal/mol) and in water ($\Delta E_{B\text{-}C}$ (H_2O) = 6.5 kcal/mol) (Table 3).

Table 1. Energy values of the conformers and the rotational transition states of **1** in the *vacuum*.

	Energy (Hartrees)	$\Delta E^{\neq}$ (Hartrees)	$\Delta E^{\neq}$ (kcal/mol)
Conformer *A*	-1566.25679		
TS *A-B*	-1566.21648	0.04031	25.3
Conformer *B*	-1566.25709		
TS *B-C*	-1566.21653	0.04056	25.5
Conformer *C*	-1566.25741		

Table 2. Energy values of the conformers and the rotational transition states of **1** in $CHCl_3$ and H_2O.

Solvent		Energy (Hartrees)	$\Delta E^{\neq}$ (Hartrees)	$\Delta E^{\neq}$ (kcal/mol)
$CHCl_3$	Conformer *A*	-1566.29762		
	TS *A-B*	-1566.25949	0.03813	23.9
	Conformer *B*	-1566.29794		
	TS *B-C*	-1566.25959	0.03835	24.1
	Conformer *C*	-1566.30399		
H_2O	Conformer *A*	-1566.30818		
	TS *A-B*	-1566.27078	0.03740	23.5
	Conformer *B*	-1566.30856		
	TS B-C	-1566.27093	0.03763	23.6
	Conformer *C*	-1566.31886		

Table 3. Energetic gap among the different conformers of **1** in the *vacuum*, $CHCl_3$ and H_2O.

	ΔE_{A-B} (kcal/mol)	ΔE_{B-C} (kcal/mol)
Vacuum	0.19	0.20
$CHCl_3$	0.20	3.8
H_2O	1.46	6.5
	$\Delta E^{\neq}_{A-B}$ (kcal/mol)	$\Delta E^{\neq}_{B-C}$ (kcal/mol)
Vacuum	25.3	25.5
$CHCl_3$	23.9	24.1
H_2O	23.5	23.6

The higher polarity of conformer *C* (μ_C = 2.26 Debye) is likely responsible for its stabilization in polar solvents. Importantly, all the activation energy values ($\Delta E^{\neq}$) slightly decrease with the polarity of the solvent, but they resulted still too high to allow the conformers interconversion. These results suggest the presence of two stable conformers (*B* and *C*), which are not in conformational exchange one with each other. However, geometry optimization show that steric effects may be relevant in each conformer to disfavor aggregation tendency of **1**.

Hence, such encouraging preliminary theoretical data prompted us to synthesize this new phenothiazinium salt and to explore its properties in solution.

Synthesis

The easiest strategy to prepare phenothiazinium salts involves the oxidation of phenothiazine by iodine.[34,35] However, it is widely known that I_2 may create problems in the nature of the counterion,[36] because the oxidation product of phenothiazine (Scheme 1, 1st step) is a salt having a molecular formula $[(PTZ)^+I^-]_2{\cdot}3I_2{\cdot}2H_2O$, thus it is composed of two phenothiazinium cations, two iodide counterions, three molecules of iodine and two molecules of water. For this reason, in this work, anionic exchange with chloride was performed after each reaction to avoid ambiguous results in terms of yield.

The first step to synthesize **1** required the synthesis of the monosubstituted product (Scheme 1, steps 2 and 3). Therefore, 3-(*N*-methyl-*N*-phenylamino)phenothiazinium was prepared, using exactly two equivalents of the proper aromatic amine and stirring the mixture until the substrate was completely consumed, as checked by TLC analysis. The reaction was slower than that with aliphatic amines, but no side products (such as the disubstituted derivative) were detected, making the purification step very easy. On the other hand, double substitution resulted in a difficult task: even if the synthesis of 3,7-bis(*N*-methyl-*N*-phenylamino)phenothiazinium chloride has been previously reported by Ihara and co-workers,[34] only 15% yield was achieved using 6 equivalents of *N*-methylaniline (*N*-MeAn) in MeOH.

Thus, to optimize the reaction process, in this work, the effect of the solvent, iodine addition and temperature have been investigated. Results are presented in Table 4. The choice of solvent (Table 4, entries 1-3) was limited by phenothiazinium salts solubility: summarizing, acetone resulted the worst one, while there was a slight difference between chloroform and methanol. Therefore, methanol was chosen as solvent for the following reactions, considering its relative sustainability and the easiness of the purification procedure. In fact, reactions performed in methanol showed negligible side products formation and the reaction mixture could be easily purified with few washes, instead of a 'plug' chromatography, as for reactions carried out in $CHCl_3$ or acetone. Rising the temperature from room to 53 °C (Table 4, entries 3 and 4) increased the yield from 21% to 33%, while no variation was observed adding one equivalent of molecular iodine (Table 4, entries 3 and 5).

The one-pot approaches have been already reported[37] and we tested the more recent procedure for ethylene blue synthesis. However, with *N*-methylaniline as nucleophile, such practical procedure was not very successful. Indeed, product purification required a time-consuming chromatography column. To reduce the amount of *N*-methylaniline, rendering the purification easier without diminishing the necessary proton scavenging, a non-nucleophilic strong base was added. Triethylamine - volatile and therefore relatively easy to remove - and carbonates were tested (Table 5). With the addition of two equivalents of triethylamine as a base, reaction time (based on the substrate disappearance on the TLC plate) was dramatically reduced, even if the yield increased only slightly (Table 5, entry 2 *vs*.1). Increasing the amount of Et_3N to 4 eqs. raised up the yield to 41% with a parallel reduction in reaction time (Table 5, entry 3).

Table 4. Synthesis of **1**. Conditions: $[(PTZ)^+I^-]_2{\cdot}3I_2{\cdot}2H_2O$ 0.05 M and *N*-methylaniline 0.3 M, 93 h.

entry	Solvent	Temp °C	Purification procedure[a]	Yield[b] %
1	Acetone	r.t.	A	2
2	$CHCl_3$	r.t.	A	19
3	MeOH	r.t.	B	21
4	MeOH	53	C	33
5[c]	MeOH	r.t.	D, A	21

[a] Purification procedures: A) the crude product was purified by a 'plug' chromatography on basic Al_2O_3 (activated, Brockmann I; eluent: ethyl acetate/methanol 9:1 v/v); B) the precipitate formed during the reaction was filtered and washed with a small amount of cold methanol; C) the reaction mixture was diluted with dichloromethane to 100 ml, extracted with 0.1 M aqueous HCl (2 x 100 ml) and washed with water until neutrality. The product was crystallized from dichloromethane/diethyl ether and washed with 10 ml of 2-propanol; D) the reaction mixture was diluted to 100 ml, extracted with 0.1 M HCl and washed with water to neutral pH. [b] Isolated yield, after purification. [c] One equivalent of I_2 added after 72 h.

Table 5. Synthesis of **1** with added bases. Conditions: $[(PTZ)^+I^-]_2 \cdot 3I_2 \cdot 2H_2O$ 0.05 M and *N*-methylaniline 0.3 M in MeOH, at room temperature.

entry	Added base (eqs.)	Time (hours)	Purification procedure[a]	Yield[b] %
1	none	93	A	21
2	Et_3N (1.7)	23	F	25
3	Et_3N (4)	3	F	41
4	Li_2CO_3 (4)	3	E	38
5	Na_2CO_3 (4)	3	E	71
6	K_2CO_3 (4)	3	E	38
7[c]	Cs_2CO_3 (4)	3	E	11

[a] Purification procedures: A) the crude product was purified by a 'plug' chromatography on basic Al_2O_3 (activated, Brockmann I; eluent: ethyl acetate/methanol 9:1 v/v); E) the crude product was purified by a 'plug' on basic Al_2O_3 (activated, Brockmann I) with $CHCl_3$ as eluent; F) at the end of the reaction the solvent was removed by rotavapor. The crude product was dissolved in dichloromethane, extracted with 0.1 M HCl (2x100 ml) and washed with water until neutral. [b] Isolated yield, after purification.

However, in both reactions the purification was still the bottleneck since neutralization of the mixture with HCl and 'plug' chromatography were needed to isolate the product.

Above all, reactions performed using carbonates as non-nucleophilic bases resulted the best choice in terms of yields and purification procedure. In fact, with carbonates extraction with HCl was not required and 71% yield was obtained using Na_2CO_3 (Table 5, entry 5). However, the other carbonate salts were not as successful as sodium: specifically, both lithium and potassium carbonates resulted in 38% of product formation (Table 5, entries 4 and 6) while cesium was even less effective (Table 5, entry 7). Therefore, the amount of the isolated product resulted highly dependent on the counterion, even if there was no trend between cation size and yield.

Such result prompted us to reconsider also the *N*-methylaniline excess, since it had no longer to act as a base. However, reactions performed using less amine amounts did not cause the expected results. Indeed, two equivalents were not enough to ensure double substitution (Table 6, entry 1), while three or four equivalents had almost the same -and not successful- outcome (Table 6, entries 2 and 3). Thus, six equivalents remained the best choice (Table 6, entry 4).

Furthermore, increasing the temperature from room to reflux decreased yield (with 4 eqs. of *N*-methylaniline and 4 Na_2CO_3 equivalents) from 57% to 27%.

Aggregation of MB and 3,7-bis(*N*-methyl-*N*-phenylamino)phenothiazinium chloride in solution: UV-Vis study.

To confirm DFT predictions, self-aggregation of **MB** and **1** was investigated using UV-Vis spectroscopy in organic solvents and in different aqueous solutions. It is worth mentioning that there are numerous UV-Vis spectroscopy studies on **MB** aggregation but results are frequently inconsistent and sometimes contradictory.[38-40]

Table 6. Synthesis of 1 with different *N*-methylaniline equivalents. Conditions: $[(PTZ)^+I^-]_2 \cdot 3I_2 \cdot 2H_2O$ 0.05 M 4 equivalents Na_2CO_3 in MeOH at room temperature.

entry	*N*-MeAn (eqs.)	Time (hours)	Purification procedure[a]	Yield[b] %
1	2	3	E	7
2	3	3	E	55
3	4	3	E	57
4	6	3	E	71

[a] The crude product was purified by a 'plug' on basic Al_2O_3 (activated, Brockmann I) with a $CHCl_3$ as eluent. [b] Isolated yield, after purification.

For both dyes, no spectral variations were observed in organic solvents changing their concentration in the range $10^{-7} \div 10^{-4}$ M, while spectral changes in water were exclusively observed with **MB** (Fig. S5). In particular, the band due to the dimeric species (605 nm) increased in intensity with increasing dye concentration, at the expense of the monomeric form (664 nm) and the observed blue shift was attributed to the formation of H-aggregates.[41,42] Conversely, according with DFT calculations, dimerization was not detected for **1**, since no spectral variation was recorded upon increasing dye concentration up to 10^{-4} M. Such behaviour has been confirmed also changing the ionic strength of the aqueous media (Figures 3-4).[43,44] Spectra recorded in 1 M aqueous NaCl solution showed that **MB** dimerization was promoted while no effects were observed for **1**, indicating that aggregation was prevented at concentrations up to 10^{-4} M by phenyl units.

However, the nature of the salt used to increase the ionic strength showed a large influence on the aggregation phenomena. As a matter of fact, aqueous solutions of $NaBF_4$ 1 M (Figure S6) or $NaClO_4$ 1 M (Figure 5) led to the formation of the trimeric species of **MB**, having a maximum at 565 nm,[45] and significant variations have been also detected for **1**, which spectrum gradually red-shifted (Figure 6).

The different aggregation behavior of the two phenothiazinium dyes is likely due to their structural differences: **MB**, being planar, gives rise to the formation of H-aggregates, while phenyl groups of **1** may be accommodated perpendicularly to the polycyclic ring, thus making easier the J-type aggregation (that is consistent with the red shift of the absorption spectrum and with the different conformers predicted with DFT calculations).

Furthermore, association appeared mainly driven by hydrophobic interactions and it resulted strongly dependent on the ionic strength and on the nature of the salt used. Thus, experiments showed that hydrophobic anions, *i.e.* BF_4^- and ClO_4^-, increased the self-aggregation tendency of the dyes.[44]

Surprisingly, pH variations did not affect the aggregation equilibrium of both dyes. Thus, spectral changes observed for **1** are likely due to its low solubility in highly acidic as well as in highly basic media (Figure S7).

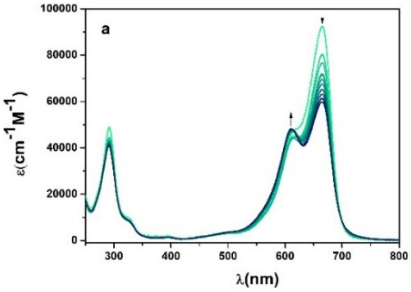

Figure 3. UV-Vis spectra in aqueous 1 M NaCl solutions of **MB**; dye concentration in the range 10^{-6}÷ 10^{-5}M).

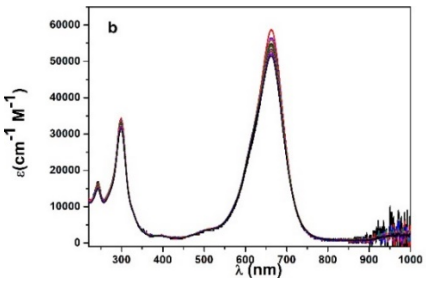

Figure 4. UV-Vis spectra in aqueous 1 M NaCl solutions of **1**; dye concentration in the range 10^{-6}÷ 10^{-5}M).

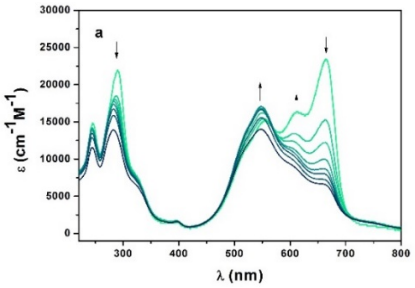

Figure 5. UV-Vis spectra in 1 M $NaClO_4$ aqueous solutions of **MB**; dyes concentration in the range 10^{-6}÷10^{-5}M.

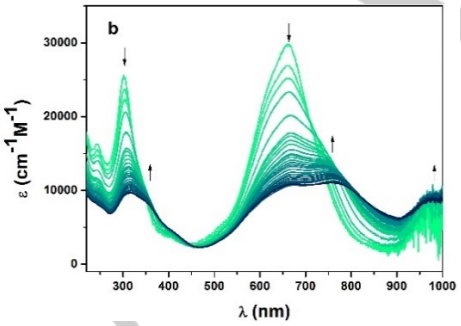

Figure 6. UV-Vis spectra in 1 M $NaClO_4$ aqueous solutions of **1**; dyes concentration in the range 10^{-6}÷10^{-5}M.

From spectral data, a dimer dissociation constant for the monomer-dimer equilibrium of **MB** in water of $2.4 \cdot 10^{-4}$ M has been calculated (Kd, see Supporting Information), and it is in line with previously reported values.[35,46-48] Dissociation constants were also evaluated, at room temperature, increasing the ionic strength with NaCl (see Supporting Information).

^{1}H NMR

MB molar extinction coefficient prevented UV-vis study at concentrations higher than 10^{-4} M, thus ^{1}H NMR experiments has been performed. Also ^{1}H NMR spectra of **MB** in D_2O appeared significantly affected by concentration (Figure 7). In particular, a large shielding effect was observed increasing **MB** concentration, confirming the establishment of π interactions among the molecules in solution. In order to measure the size of the aggregates, diffusion ordered ^{1}H NMR experiments were carried out (see Supporting Information). The correlation between the obtained hydrodynamic radius (Rh) and the **MB** concentration is shown in Figure S12. At the lowest concentration studied ($2 \cdot 10^{-5}$ M) a Rh value of 4.3 Å has been observed while at higher concentrations, a maximum value of 12.3 Å could be extrapolated. To fully understand these data, the size of the monomer and dimer species of **MB** have been measured with DFT models (Fig. S14). Values of 4.1 Å and 6.2 Å were calculated for the Rh of monomeric and dimeric forms, respectively.

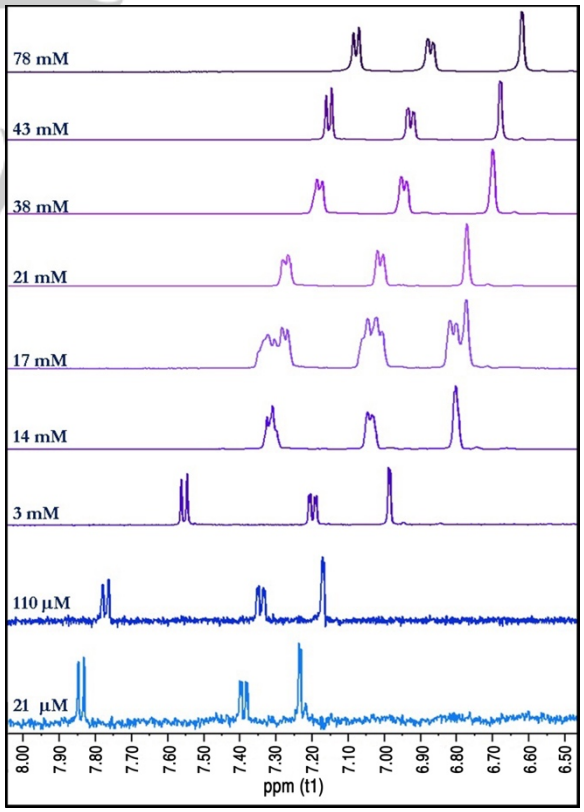

Figure 7. Aromatic region in ^{1}H NMR spectra of **MB** in D_2O at different concentrations.

Based on the comparison among these experiments, the monomer-dimer equilibrium apparently occurs at **MB** concentration below to $5 \cdot 10^{-3}$ M, then high-order aggregates form. The same experiments have been performed with **1**. The hydrodynamic radius in D_2O ($2.3 \cdot 10^{-4}$ M, at 298 K) was 5.2 Å, which is consistent with the size of the molecule measured with DFT calculations. Such evidence confirms the assumptions based on the UV-vis experiments in water, where in the analysed concentration range ($10^{-7} \div 10^{-4}$ M) no association was detected, indicating that **1** remains in its monomeric form. However, the low solubility in D_2O made no possible experiments at concentration higher than 10^{-4} M, thus $CDCl_3$ was used to study **1** aggregation. Hence, ^{1}H NMR spectra were collected from 10^{-4} M to 10^{-2} M (Figure 8). Changes in signals number (there are more signals than in D_2O) and shape (they become broader with increasing concentrations, but only some of them change chemical shift) have been detected. Interestingly, two different methyl signals have been observed, likely indicating the presence of 2 conformers in solution. The relative intensities of such signals suggest a different distribution of the two rotamers, whose interconversion might be promoted by water or acid traces. Further NMR and computational experiments will be necessary to completely clarify this behaviour. However, as previously discussed, it can be assumed that the spectrum recorded at $1.0 \cdot 10^{-4}$ M is related to the monomer species and apparently no aggregates form up to $1.0 \cdot 10^{-3}$ M.

Conversely, broad signals recorded at concentrations higher than $1.0 \cdot 10^{-3}$ M are reasonably due to PTZ^+ self-aggregation. The diffusion ordered ^{1}H NMR experiments showed only slight variation in the hydrodynamic radii, even if the formation of high-order aggregates may be expected (Table S3).

All the data depicted an intriguing picture, which involves the dynamic aggregation equilibrium of the dyes, where high-order aggregates may be involved, together and the differences in geometrical conformers.

Cyclic Voltammetry

Phenothiazinium salts are known to act as electron acceptor molecules, but it must be considered that also electrochemical properties are influenced by dye concentration and ionic strength, because of aggregation. Therefore, **MB** and **1** electrochemical behavior has been investigated at different dye concentrations ($10^{-5} \div 10^{-4}$ M) both, in organic solvents and aqueous media.

No important electrochemical variations were observed in acetonitrile, as expected from the corresponding UV-visible results in the same conditions (Figures S17 and S18). In fact, one reversible reduction process was observed for both dyes, with significant difference in half wave potential (Figure 9, Table S4). Notably, reduction process in **1** occurs at lower potential than in **MB**.

Conversely, significant variations in the electrochemical profile have been observed using phosphate buffer as the solvent (Figure 10): at [**MB**] = 10^{-5} M one reversible reduction process centered at -260 mV has been observed, while at higher **MB** concentration an additional wave has been detected, reasonably associated with the formation of the dimeric form in solution.

Moreover, the additional process occurs at potentials very close to 0 V, suggesting a more favorable reduction of the dimer with respect to the monomer. Conversely, voltammogram obtained for **1** (Figure S19) was not of easy interpretation, but this result is consistent with the intriguing picture emerged for such phenothiazinium salt in solution.

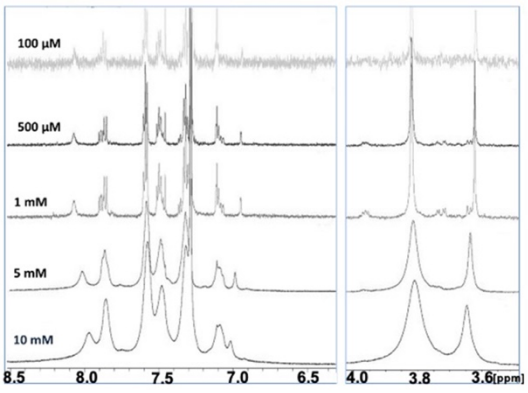

Figure 8. ^{1}H NMR spectra of **1** in $CDCl_3$ at different concentrations.

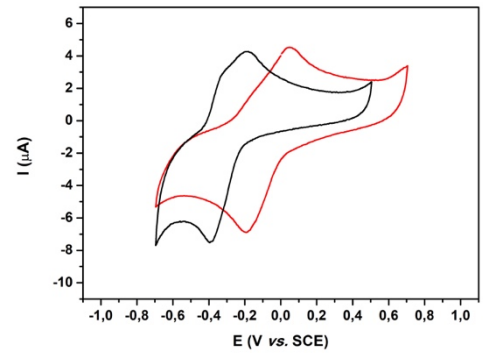

Figure 9. Cyclic voltammetry (100 mV/s) in CH_3CN/0.1 M TBAP of **MB** (black line) and **1** (red line).

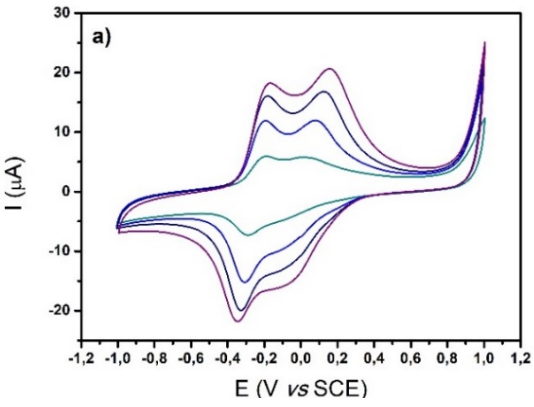

Figure 10. Cyclic voltammetry in 0.1 M phosphate buffer (pH=7.2) for **MB**; concentration range $10^{-5} \div 10^{-4}$ M.

Conclusions

Due to the important potential applications of phenothiazinium salts besides **MB**, the research of new PTZ^+ derivatives is required, in order to limit the aggregation tendency of these salts usually occurring in solution. In fact, aggregation restricts the usage of this compounds in many areas. Hence, in this paper we proposed a reliable synthetic procedure to obtain a properly substituted PTZ^+ salt, *i.e.* 3,7-bis(*N*-methyl-*N*-phenylamino)phenothiazinium chloride, in good yields. Such reaction can be actually used as a model to prepare also differently substituted PTZ^+ derivatives.

As predicted by DFT models, the aggregation aptitude of **1** resulted much lower than that of **MB**. Indeed, phenyl groups in positions 3 and 7 can be accommodated perpendicularly, in equatorial-like conformation or one perpendicular and the other in the equatorial-like conformation with respect to the PTZ^+ core, giving rise to the formation of different conformers in solution. UV-vis and ^{1}H NMR spectroscopies confirmed that the steric hindrance originated by such groups makes **1** remaining in its monomeric form up to concentrations of $1.0 \cdot 10^{-3}$ M in organic solvents and water. Conversely, aggregation is promoted at lower concentration, in the presence of high ionic strength. It is worth mentioning that the dimeric form of **MB** was already observed at concentration lower than 10^{-4} M in aqueous solutions and also trimeric species were detected at concentration of $5 \cdot 10^{-3}$ M.

Moreover, the presence of two phenyl groups bounded on the PTZ core implies a significant variation of the reduction potential of the molecule, that can be reduced at a more accessible potential than **MB**.

Hence, the introduction of phenyl rings directly bounded on the PTZ^+ resulted in a useful strategy for preventing aggregation of phenothiazinium salts, thus opening new opportunities in the application of such molecules in DSSCs and in the photodynamic therapy field.

Experimental Section

Materials and instruments

All commercial reagents and solvents were purchased from Sigma-Aldrich, VWR or Fluka, at the highest degree of purity available, and were used without any further purification. The absorption spectra were recorded with a UV-Vis 2450 Shimadzu spectrophotometer. ^{1}H NMR experiments were carried out using a Bruker Advance (600.13 MHz) equipped with an inverse broad band probe with z-gradients and all data were processed with TopSpin software. MS-ESI analyses have been performed with a LC-MSD-trap-SL ESI+FI. Electrochemical measurements were performed using Palmsens potentiostat with PS-Trace software. DFT calculations have been performed with Gaussian 16 rev. A03.[49]

Synthesis of 3-(methylphenylamino)phenothiazinium triiodide

N-methylaniline (1.38 mmol) in 2 ml methanol was added dropwise to a solution of 0.69 mmol phenothiazinium salt, $[(PTZ)^+I^-]_2 \cdot 3I_2 \cdot 2H_2O$ in 10 ml of the same solvent. The reaction mixture was stirred at room temperature, monitored by thin-layer chromatography on silica gel (eluent, 3% aqueous NH_4OAc/CH_3OH 1:17 v/v). A 15 hrs reaction time was necessary to complete the substrate consumption. The resulting product was collected by filtration and washed with diethyl ether. 206 mg were obtained (0.30 mmol; yield, 44%). UV-Vis in CH_3OH [λ_{max}, nm (ε, $M^{-1}cm^{-1}$)]: 582 (21800); 437 (17900); 303 (37400). Anal. Calcd for $C_{19}H_{15}I_3N_2S$: C, 33.36%; H, 2.21%; N, 4.09%; S, 4.69%. Found: C, 32.89%; H, 2.15%; N, 4.09%; S, 4.72%. (ESI$^+$) 303.20 ([M- X^-]$^+$, $C_{19}H_{15}NS^+$ requires 303.41 (Figure S1). ^{1}H NMR in DMSO (Figure S2): δ 8.46-8.32 (s broad, 2H), δ 8.14-8.02 (d, J = 9.46 Hz, 1H), δ 8.02-7.87 (m broad, 2H), δ 7.80-7.51 (m broad, 6H), δ 7.33-7.15 (d, J = 9.07 Hz, 1H), δ 3.98-3.85 (s, 3H).

Synthesis of 3,7-bis(*N*-methyl-*N*-phenylamino)phenothiazinium salt (1)

a) General procedure. The reaction was performed modifying the procedure reported for preparation of 3,7-bis(*N*,*N*-dialkylaminophenyl)phenothiazines.[36] A known amount of *N*-methylaniline in the appropriate solvent was added dropwise to a solution of $[(PTZ)^+I^-]_2 \cdot 3I_2 \cdot 2H_2O$, in the same solvent, at different concentrations. The reaction mixture was monitored by TLC on silica gel (eluent: 3% aqueous NH_4OAc/CH_3OH 1:17 v/v) and stirred in the dark, until the corresponding initially formed mono- substituted product was consumed. The disubstituted product was isolated and purified by different procedures, as reported in Tables 4-6. After purification, the corresponding chloride salt was obtained by anion exchange resin (eluent $CHCl_3/CH_3OH$ 1:1 v/v). The product has been easily crystallized from dichloromethane/hexane mixture. Purity was checked by LC-mass spectra and confirmed by elemental analysis. Different runs were performed changing one reaction condition at a time. The anion was generally chloride, except in Table 1, entry 3, where triiodide was the counterion, as demonstrated by elemental analysis and ^{1}H NMR spectrum (vide infra).

b) with base added and different reagents ratio. Bases different from the nucleophile *N*-methylaniline were added, to facilitate deprotonation and work-up. Different reagents ratios were also used in the presence of added sodium carbonate (see Supporting Information).

c) one-pot synthesis.[50] A solution of *N*-MeAn (2.72 ml, 25.1 mmol) in 3 mL of CH_2Cl_2 was added dropwise to a stirred suspension of phenothiazine (0.5 g, 2.51 mmol) and iodine (1.91 g, 7.53 mmol) in dichloromethane (6 ml). The reaction was allowed to reflux until the corresponding monosubstituted product was consumed. After 9 h, the reaction was stopped and the product isolated by basic Al_2O_3 'plug' (activated, Brockmann I; eluent: chloroform). The pure compound was passed through a strongly basic anion exchange resin in order to replace iodide with chloride (eluent: $CHCl_3/CH_3OH$ 1:1 v/v). The product was crystallized from dichloromethane/diethyl ether (599 mg, 1.25 mmol, yield, 50%).

3,7-bis(*N*-methyl-*N*-phenylamino)phenothiazinium triiodide (Table 4, entry 3)

UV-Vis in CH_3OH [λ_{max}, nm (ε, $M^{-1}cm^{-1}$)]: 652 (76400); 296 (45800); Anal. Calcd for $C_{26}H_{22}I_3N_3S$: C, 39.57%; H, 2.81%; N, 5.32%; S, 4.06%; Found: C, 39.94%; H, 2.30%; N, 5.34%; S, 6.38%; m/z (ESI$^+$) 408.27 ([M-X^-]$^+$, $C_{26}H_{22}N_3S^+$ requires 408.15); ^{1}H NMR in $CDCl_3$: δ 7.93-7.88 (d, J = 9.59 Hz, 2H), δ 7.63-7.57 (m, 4H), δ 7.54-7.47 (m, 4H), δ 7.39-7.35 (m, 4H), δ 7.16-7.11 (dd, J_1 = 9.59 Hz, J_2 = 2.51 Hz, 2H).

3,7-bis(*N*-methyl-*N*-phenylamino)phenothiazinium chloride

UV-Vis in CH_3OH [λ_{max}, nm (ε, $M^{-1}cm^{-1}$)]: 652 (76400); 296 (45800); Calcd for $C_{26}H_{22}ClN_3S \cdot 0.5\ CH_3OH$: C, 69.19; H, 5.26; N, 9.13; S, 6.97; Found: C, 69.57; H, 5.45; N, 8.60; S, 6.92; m/z (ESI$^+$) 408.27 ([M- X^-]$^+$, $C_{26}H_{22}N_3S^+$ requires 408.15)

Elemental analyses for different samples of 3,7-bis(methylphenylamino)phenothiazinium chloride: Calcd. for $C_{26}H_{22}N_3SCl \cdot 0.5\ CH_3OH$: C 69.28%, H 5.22%, N 9.15%, S 6.97%. Found: C 70.35%, H 5.43%, N 8.77%, S 6.82% for sample in Table 5, entry 4; C 70.00%, H 5.54%, N 8.71%, S 6.92% for sample in Table 5, entry 5; C 69.57%, H 5.45%, N 8.60%, S 6.92% for sample in Table 5, entry 6; C 70.35%, H 5.43%, N 8.77%, S 6.82% for sample in Table 6, entry 3.

UV-Vis investigation

Self-aggregation of dyes in organic solvents (dichloromethane, dimethyl sulfoxide, ethanol, methanol), water, aqueous solutions of different salts ($NaCl$, $NaBF_4$, $NaClO_4$) and of different pH values (0, 3, 7.5, 12) has been investigated with different concentrations in the range 10^{-7} to 10^{-4} M. Cuvettes with 1 cm and 1 mm path length have been used.

NMR investigation: Diffusion order and CPMG experiments

The hydrodynamic radii of the aggregates in D_2O were investigated by gradient-dependent ^1H NMR diffusion experiments. Since molecular diffusion depends on the size and the shape of the molecules, on the temperature and on the viscosity of the solution, all the measurements have been carried out at constant temperature (300 K), in order to remove the dependence on the latter two variables. Dioxane was used as internal standard. Details can be found in Supporting Information.

Computational calculations

Fully geometry optimizations calculations were performed using Gaussian 16, with Density Functional Theory approach, using B3LYP or WB97XD functional and 6-31G+(d,p) basis set.[49]

Cyclic voltammetry measurements

Cyclic voltammetries were carried at different dyes concentrations in organic solvent (anhydrous acetonitrile) and aqueous media (phosphate buffer 0.1 M, pH = 7.2). 0.1 M tetrabutylammonium perchlorate (TBAP) was chosen as supporting electrolyte in acetonitrile. As reference, working and counter electrodes saturated calomel (SCE), glassy carbon (GC) and Pt wire were used, respectively.

Acknowledgements

Prof. Maria Pia Donzello, University of Rome “Sapienza” is acknowledged for elemental analysis.

Keywords: phenothiazinium • equilibrium • monomer-dimer • aggregation

[1] P. V. Kamat, N. N. Lichtin, J. *Phys. Chem*. **1981**, 85, 814-818.
[2] C. Lal, *J. Power Sources* **2007**, *164*, 926-930.
[3] A. Malviya, P. P. Solanki, *Renew. Sust. Energ. Rev*. **2016**, *59*, 662-691.
[4] See as example: a) K. K. Hussain, J.-M. Moon, D.-Su Park, Y.-B Shim, *Electroanalysis* **2017**, *29*, 2190-2199; b) J. Ye, P. R. Baldwin, *Anal. Chem.* **1988**, *60*, 2263-2268
[5] J. Ma, Z. Zhang, M. Yang, Y. Wu, X. Feng, L. Liu, X. Zhang, Z. Tong, *Micropor. Mesopor. Mat*. **2016**, *221*, 123-127.
[6] L. Cuia, M. Lua, Y. Lib, B. Tanga, C.-Y. Zhanga, *Biosens. Bioelectron*. **2018**, *102*, 87-93.
[7] E. M. Tuite, B. Nordén, *Spectrochim. Acta A* **2018**, *189*, 86-92.
[8] J. J. Nogueira, M. Oppel, L. González, *Angew. Chem. Int. Ed*. **2015**, *54*, 4375-4378.
[9] E. Tuite, B. Norden, *J. Am. Chem. Soc*. **1994**, *116*, 7548-7556.
[10] M. Wainwright, J. Antczak, M. Baca, C. Loughran, K. Meegan, *J. Photochem. Photobiol. B* **2015**, *150*, 38-43.
[11] A. Gollmer, A. Felgenträger, W. Bäumler, T. Maischa, A. Späth, *Photochem. Photobiol. Sci*. **2015**, *14*, 335-351.
[12] M. Wainwright, K. Meegan, C. Loughran, *Dyes Pigm*. **2011**, *91*, 1-5.
[13] S. A. Gorman, A. L. Bell, J. Griffiths, D. Roberts, S. B. Brown, *Dyes Pigm*. **2006**, *71*, 153-160.
[14] J. Tardivo, A. Del Giglio, C. De Oliveira, D. Gabrielli, H. Junquiera, D. Tada, D. Severino, R. Turchiello, M. Baptista, *Photodiagn. Photodyn. Ther*. **2005**, *2*, 175-191.
[15] G. Rodriguez, L. Ferreira, M. Wainwrigh, G. Braga, *J. Photochem. Photobiol. B* **2012**, *116*, 89-94.
[16] See as example: a) M. Wainwright, *Photodiagn. Photodyn. Ther*. **2005**, *2*, 263-272; b) A. Coronel, J. Catalán-Toledo, H. Fernández-Jaramillo, P. Godoy-Martínez, M. E. Flore, I. Moreno-Villoslada, *Dyes Pigm*. **2017**, *147*, 455-464.
[17] B. Lambrecht, H. Mohr, J. Knulver-Hopf, H.Schimtt, *Vox Sang*. **1991**, *60*, 207-213.
[18] A. Elikaei, Z. Sharifi, S. M. Hosseini, H. Latifi, M. Kamaran, M. Hosseini, *Iran. J. Microbiol*. **2014**, *6*, 41-45.
[19] B. Varga, Á. Csonka, A. Csonka, J. Molnár, L. Amaral, G. Spengler, *Anticancer Res*. **2017**, *37*, 5983-5993.
[20] See as example: a) R. Schölin, M. Quintana, E. M. J. Johansson, M. Hahlin, T. Marinado, A. Hagfeldt, H. Rensmo, *J. Phys. Chem. C* **2011**, *115*, 19274-19279; b) A. Mishra, M. K. R. Fischer, P. Bäuerle, *Angew. Chem. Int. Ed.* **2009**, *48*, 2474-2499; c) X. Zarate, M. Saavedra-Torres, A. Rodriguez-Serrano, T. Gomez, E. Schott, *J. Comput. Chem.* **2018**, *39*, 685-698.
[21] M. Kostka, P. Zimcik, M. Miletin, P. Klemera, K. Kopecky, Z. Musi, *J. Photoch. Photobio. A* **2006**, *178*, 16-25.
[22] M. Gardner, A. J. Guerin, C. A. Hunter, U. Michelsen, C. Rotger, *New J. Chem.* **1999**, *23*, 309-316.
[23] C. A. Hunter, C. M. R. Low, C. Rotger, J. G. Vinter, C. Zonta, *Proc. Natl. Acad. Sci. USA* **2002**, *99*, 4873-4876.
[24] S. Berardi, V. Conte, G. Fiorani, B. Floris, P. Galloni, *J. Organomet. Chem*. **2008**, *693*, 3015-3020.
[25] A. Coletti, S. Lentini, V. Conte, B. Floris, O. Bortolini, F. Sforza, F. Grepioni, P. Galloni, *J. Org. Chem*. **2012**, *77*, 6873-6879.
[26] S. Bertini, A. Coletti, B. Floris, V. Conte, P. Galloni, *J. Inorg. Biochem*. **2015**, *147*, 44-53.
[27] M. Tiravia, A. Vecchi, F. Sabuzi, G. Pomarico, A. Coletti, B. Floris, V. Conte, P. Galloni, *J. Porphyrins Phtalocyanines* **2016**, *20*, 421-428.
[28] F. Sabuzi, S. Lentini, F. Sforza, S. Pezzola, S. Fratelli, O. Bortolini, B. Floris, V. Conte, P. Galloni, *J. Org. Chem*. **2017**, *82*, 10129-10138.
[29] F. Sabuzi, V. Armuzza, V. Conte, B. Floris, M. Venanzi, P. Galloni, E. Gatto, *J. Mater. Chem. C* **2016**, *4*, 622-629.
[30] F. Sabuzi, M. Tiravia, A. Vecchi, E. Gatto, M. Venanzi, B. Floris, V. Conte, P. Galloni, *Dalton Trans*. **2016**, *45*, 14745-14753.
[31] M. Bonomo, F. Sabuzi, A. Di Carlo, V. Conte, D. Dini, P. Galloni, *New J. Chem*. **2017**, *41*, 2769-2779.
[32] F. Bettanin, T. A. de Carvalho Fontinelles, C. D. Maciel, L. G. Dias, M. D. Coutinho-Neto, P. Homem-de-Mello, *Theor. Chem. Acc*. **2015**, *134*, 1-11.
[33] L. M. da Costa, S. R. Stoyanov, S. Gusarov, X. Tan, M. R. Gray, J. M. Stryker, R. Tykwinski, J. W. de M. Carneiro, P. R. <seidl, A. Kovalenko, *Energy Fuels* **2012**, *26*, 2727-2735.
[34] Y.-T. Lu, C. Arai, J.-F. Ge, W.-S. Ren, M. Kaiser, S. Wittlin, R. Brun, J.-M. Lu, M. Ihara, *Dyes Pigm*. **2011**, *89*, 44-48.
[35] K. Bergmann, C. T. O'Konski, *J. Phys. Chem*. **1963**, *67*, 2169-2177.
[36] L. Strekowski, D. F. Hou, R. L. Wydra, *J. Heterocycl. Chem.* **1993**, *30*, 1693-1695.

[37] a) J. A. Cody, C. S. Larrabee, M. D. Clark, S. Hlynchuk, J. A. Tatum, *Tetrahedron Lett*. **2012**, *53*, 4896-4899; b) M. Wainwright, N. J. Grice, L. E.C. Pye, *Dyes Pigm*. **1999**, *42*, 45-51

[38] C. Parkanyi, C. Boniface, J. J. Aaron, M. Maafi, *Spectrochim. Acta A* **1993**, *49*, 1715-1725.

[39] G. N. Lewis, O. Goldshmid, T. T. Magel, J. Bigeleisen, *J. Am. Chem. Soc*. **1943**, *65*, 1150-1154.

[40] K. Patil, R. Pawar, P. Talap, *Phys. Chem. Chem. Phys*. **2000**, *2*, 4313-4317.

[41] D. Liu, P. V. Kamat, *Langmuir* **1996**, *12*, 2190-2195 and references cited therein.

[42] A. Ghanadzadeh Gilani, M. Moghadam, S.E. Hosseini, M.S. Zakerhamidi, *Spectrochim. Acta A* **2011**, *83*, 100-105.

[43] O. Yazdani, M. Irandoust, J. B. Ghasemi, S. Hooshmand, *Dyes Pigm*. **2012**, *92*, 1031-1041.

[44] J. Wang, H. Wang in *Aggregation in Systems of Ionic Liquids,* Structures and Interactions of Ionic Liquids (Eds. S. Zhang, J. Wang, Q. Zhao, Q. Zhou) Springer-Verlag Berlin, **2014**, 39-77.

[45] E. Braswell, *J. Phys. Chem*. **1968**, *72*, 2477-2483.

[46] E. Rabinowitch, L. F. Epstein, *J. Am. Chem. Soc*. **1941**, *63*, 69-78.

[47] P. Mukerjee, A. K. Ghosh, *J. Am. Chem. Soc*. **1963**, *67*, 193-201.

[48] E. Braswell, *J. Phys. Chem*. **1968**, *72*, 2477-2483.

[49] Gaussian 16, Revision A.03, M. J. Frisch, G. W. Trucks, H. B. Schlegel, G. E. Scuseria, M. A. Robb, J. R. Cheeseman, G. Scalmani, V. Barone, G. A. Petersson, H. Nakatsuji, X. Li, M. Caricato, A. V. Marenich, J. Bloino, B. G. Janesko, R. Gomperts, B. Mennucci, H. P. Hratchian, J. V. Ortiz, A. F. Izmaylov, J. L. Sonnenberg, D. Williams-Young, F. Ding, F. Lipparini, F. Egidi, J. Goings, B. Peng, A. Petrone, T. Henderson, D. Ranasinghe, V. G. Zakrzewski, J. Gao, N. Rega, G. Zheng, W. Liang, M. Hada, M. Ehara, K. Toyota, R. Fukuda, J. Hasegawa, M. Ishida, T. Nakajima, Y. Honda, O. Kitao, H. Nakai, T. Vreven, K. Throssell, J. A. Montgomery, Jr., J. E. Peralta, F. Ogliaro, M. J. Bearpark, J. J. Heyd, E. N. Brothers, K. N. Kudin, V. N. Staroverov, T. A. Keith, R. Kobayashi, J. Normand, K. Raghavachari, A. P. Rendell, J. C. Burant, S. S. Iyengar, J. Tomasi, M. Cossi, J. M. Millam, M. Klene, C. Adamo, R. Cammi, J. W. Ochterski, R. L. Martin, K. Morokuma, O. Farkas, J. B. Foresman, D. J. Fox, Gaussian, Inc., Wallingford CT, 2016.

[50] F. Andreani, P. Costa Bizzarri, C. Della Casa, M. Fiorini, E. Salatelli, *J. Heterocycl. Chem*. **1991**, *28*, 295-299.

10.1002/ejoc.201900504

WILEY-VCH

Table of Contents

FULL PAPER

Design and synthesis optimization of 3,7-bis(N-methyl-N-phenylamino)phenothiazinium chloride is proposed. A detailed analysis using DFT calculations, UV-vis, ^{1}H NMR and electrochemical studies, supporting the evidence that - differently from Methylene Blue- the aggregation is prevented up to concentration of $1.0 \cdot 10^{-3}$ M.

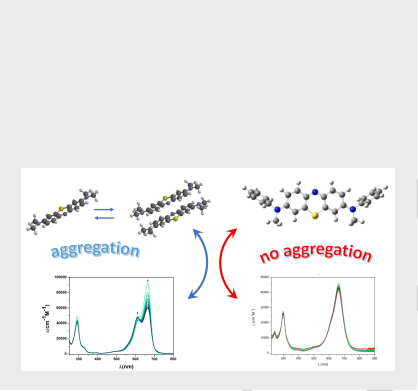

Aggregation*

*Martina Tiravia, Federica Sabuzi, Martina Cirulli, Silvia Pezzola, Graziano Di Carmine, Daniel Oscar Cicero, Barbara Floris, Valeria Conte and Pierluca Galloni**

Page No. – Page No.
3,7-bis(*N*-methyl-*N*-phenylamino)phenothiazinium salt: improving synthesis and understanding aggregation behaviour in solution